

MIMO-HSDPA ENERGY ALLOCATION OPTIMIZATION

MEHMET GORKEM ULKAR

Supervisor: Dr. M.K.Gurcan

A Thesis submitted in fulfillment of requirements for the degree of
Master of Science
Wireless Communications
of Lund University

Department of Electrical and Information Technology
Lund University
Department of Electrical and Electronic Engineering
Imperial College London
August 16, 2012

Abstract

The HSDPA-MIMO system has been developed for providing higher capacity by introducing major improvements. In HSDPA, multi orthogonal sequences are transmitted with equal energies. However, operation in frequency selective channel decreases the system throughput since the sequences are not orthogonal to each other anymore. Allocating different energies to the channels considering this phenomena increases the attainable capacity. The thesis work, which is done under Dr. Gurcan's group at Imperial College, is about presenting and simulating different optimization methods. The report starts with Margin Adaptive Allocation type which basically tries to decrease needed energy for a discrete bit rate. In order to increase the capacity more and decrease the computational complexity, another type of receiver called Successive Interference Cancellation is presented. Using total available energy more efficiently and utilizing unused energy, the capacity is immensely increased especially in the channels that have many multipath components.

Acknowledgment

Firstly, I would like to thank my thesis supervisor, Dr. Mustafa K. Gurcan, for accepting me in his invaluable research group, his guidance and support. His broad vision and motivation facilitated the progress of my project immensely, and I regard it as a privilege to work with him and his research group at Imperial College London.

Special thanks to teaching staff of Lund University Wireless Communications department for providing excellent education during my MSc degree. I want to especially thank Dr. Fredrik Rusek for his continued support.

Finally, I would like to thank my family who has always been supported and loved me.

Contents

Abstract	2
Acknowledgment	3
Contents	4
List of Figures	6
Abbreviations	7
Notation	8
Chapter 1. Introduction	9
1.1 Background	9
Chapter 2. System Model	13
2.0.1 Margin Adaptive Allocation	13
2.0.2 Successive Interference Cancellation Receiver	19
2.0.3 System Value Approach for Determining Rates	22
2.0.4 Two-Group Approach	22
Chapter 3. Capacity Simulations	24
3.1 Background	24
Chapter 4. End to End Transmission Simulations	28
4.1 Simulation Setup	28
4.2 Results	32
4.2.1 Margin Adaptive Allocation Scheme	32
4.2.2 SIC Allocation Scheme	35
4.2.3 Allocation of the Residual Energy	37
Chapter 5. Conclusion	42

List of Figures

2.1	Margin Adaptive HSDPA-MIMO System Model	14
2.2	SIC HSDPA-MIMO System Model	20
3.1	Pedestrian A Channel Results	26
3.2	Pedestrian B Channel Results	27
3.3	Vehicular A Channel Results	27
4.1	Margin Adaptive-Vehicular A-100 bits	32
4.2	Margin Adaptive-Vehicular A-1000 bits	33
4.3	Margin Adaptive-Pedestrian A-1000 bits	34
4.4	Margin Adaptive-Pedestrian B-1000 bits	35
4.5	SIC-Vehicular A-1000 bits	36
4.6	SIC-Pedestrian A-1000 bits	36
4.7	SIC-Pedestrian B-1000 bits	37
4.8	Modified SIC with Residual Allocation-Pedestrian B-1000 bits	40
4.9	Margin Adaptive with Residual Allocation-Vehicular A-1000 bits	40

Abbreviations

- HSDPA:** High Speed Downlink Packet Access
- WCDMA:** Code Division Multiple Access
- WCDMA:** Wideband Code Division Multiple Access
- UMTS:** Universal Mobile Communications System
- 3G:** Third Generation Mobile Telecommunications
- MIMO:** Multiple Input Multiple Output
- TSC:** Total Squared Correlation
- CSI:** Channel State Information
- OVSF:** Orthogonal Variable Spreading Factor
- ICI:** Inter-Code Interference
- ISI:** Intersymbol Interference
- LMMSE:** Linear Minimum Mean Square Error
- MAP:** Maximum a Posteriori
- SI:** Self Interference
- SNR:** Signal to Noise Ratio
- SNIR:** Signal to Noise and Interference Ratio
- QAM:** Quadrature Amplitude Modulation
- TTI:** Transmission Time Interval
- SIC:** Successive Interference Cancellation

Notation

A Matrix

\underline{a} Column Vector

a Scalar

$|\underline{a}|$ Norm of a column vector

$E(\cdot)$ Expectation

\otimes Kronecker Product

\mathbf{I}_N (NxN) Identity Matrix

$\underline{0}_N$ (Nx1) Zeros Matrix

$(\cdot)^T$ Transpose

$(\cdot)^H$ Hermitian

Chapter 1

Introduction

1.1 Background

THE High Speed Downlink Packet Access (HSDPA), which uses multicode wideband code division multiple access (WCDMA) as its air interface, was introduced in the Release 5 specification of the Universal Mobile Telecommunications System (UMTS) as a response to the increased downlink traffic demand [1], [2], [3]. For providing higher data peak rates, increased capacity and decreased delays HSDPA introduces major improvements namely fast link adaptation, fast hybrid automatic repeat request and fast scheduling [1]. These modifications enable users to have many high data rate 3G services such as web browsing and streaming live videos on their mobile phones.

Increasing downlink throughput is the center of the research on the HSDPA. For this aim, Multiple Input - Multiple Output (MIMO) HSDPA system [4] was introduced in the Release 7 specification of the UMTS. In HSDPA-MIMO, high speed data stream is first demuxed to different antennas and then demuxed to different lower speed data streams each transmitted by a channelization code. In Release 8, 64-QAM usage combined with MIMO was also supported for the further progress in throughput. The capacity of HSDPA-MIMO has been investigated in [5], [6] in detail. As such improvements are being developed for providing higher data rates, the fact that achievable data rates in practice is still far from the theoretical upper-bound is shown in [7] and [8]. Although the

resource allocation is highly efficient in HSDPA compared to the previous specifications, [8] emphasizes that being lower than the optimal data throughput means there is a need for future optimizations. The aim of the work currently carried out in our research group is to find some techniques to optimize data throughput in HSDPA with taking the complexity into account.

Optimizing the throughput can be done by considering many different issues such as user scheduling, signature sequence design and optimizing resource allocation. Multiuser scheduling in HSDPA is deeply studied in [9]. [10] compares the performances of conventional spreading system with different strategies in frequency selective environment. [11] obtains the sum capacity bound for binary signature sequence codes. This work is important for comparing the efficiencies of the different spreading systems. Signature sequence sets having the least total squared correlation (TSC) after the channel are accepted optimum [12]. Signature series are iteratively optimized in a way that they have the least TSC for fixed and variable transmit power conditions in [12]. [13] shows the way of finding the optimal spreading sequences for a given multipath fading channel and the algorithm allocating the transmission powers into the channel space in an optimal way. The spreading sequences found in [13] keep their orthogonality even after transmitted over the frequency selective multipath channel.

For using the algorithms showed in [13], the full channel state information (CSI) is needed at the transmitter and the receiver side. It is also important to note about CSI that many other publications about optimization of HSDPA accept the presence of CSI at the transmitter and the receiver such as [9], [11]. However, it is stated in [14] that having an accurate CSI requires lots of information exchange which is not possible practically. This is either because the it would be too much information to be transmitted frequently and/or channel state will also change before this information is being utilized [15]. In order to solve this problem HSDPA uses a set of orthogonal spreading codes called Orthogonal Variable Spreading Factor (OVSF) [16]. For HSDPA-MIMO, this set is used after weighted by precoding values and then concatenated to generate longer orthogonal spreading sequences. The first Release 7 specification had 4 precoding vectors to achieve this task [2].

As aforementioned, the precoded OVSF codes are orthogonal to each other at the transmitter. However they lose their orthogonality as they are transmitted over the frequency selective channels. The codes are correlated after the frequency selective channels and this is called inter-code interference (ICI). Moreover, multipath channels bring about intersymbol interference (ISI) by making successive symbols overlap. For making practical throughput close to the theoretical one, these effects should be reduced. Equalizers or Rake receivers are used to mitigate the effects of the frequency selective channels in CDMA based systems. In [17], it is showed that linear minimum mean square error (LMMSE) equalizers outperform Rake receivers because of the fact that Rake receivers are unaware of the noise caused by the distorted parts of different codes. LMMSE equalizers showed in [18] mitigates those effects by making the received codes orthogonal. It is also stated in [8] that LMMSE equalizers are cost-effective and low-complexity solutions and they are very close to the optimum. According to [15] and [19], maximum a posteriori (MAP) receiver is optimal but its complexity is too high for being used for frequency selective channels. Furthermore, linear zero forcing equalizers cause noise enhancement [15] and they perform worse than LMMSE equalizers. The designs of LMMSE equalizers and receivers are extensively examined in [17] and [20].

ICI and ISI together constitute self interference (SI). Linear MMSE equalizer, which is mentioned before, reduces SI. To decrease SI further, successive interference cancellation scheme can be used together with symbol or chip level linear MMSE equalizer [21]. Use of SIC at the receiver side shifts the practical capacity curve up and the gap between it and the theoretical upper bound decreases.

This paper explains different allocation schemes proposed by the research group I involve and the result of the tests of these schemes. The main type of optimization done by the group is to allocate the energies to the channels in an efficient way. For the optimization the system value maximization [22] is used which is derived from the mean square error minimization [23]. This technique allocates energies to the channels that maximize the total system value which yields maximization of the system throughput. Margin adaptive allocation presented in the next section increases the total rate by optimizing the allocation

of the given transmission power. In addition to margin adaptive loading, novel SIC system model is given in the next section. SIC-based power allocation further increases the total rate by diminishing the SI. It also eliminates the need for large matrix inversions which results in better operating performance. The report continues with the results of the capacity simulations after the system model. These simulations are for comparing algorithms mathematically without trying them in the system simulations. Chapter 4 consists of end to end transmission simulations which is simulating the whole system that includes proposed schemes.

Finally, Chapter 5 concludes the thesis.

Chapter 2

System Model

2.0.1 Margin Adaptive Allocation

This part of the report presents the process of transmitting parallel data streams for non-SIC and SIC cases. The system model for margin adaptive allocation scheme is shown in figure (2.1) [24].

Assume the multicode CDMA system shown in Fig. 1 has N_T and N_R transmitter and receiver antennas. It has also K spreading sequences and the number of channels are reduced to K^* after excluding the weak channels for a given set of spreading sequences. Each channel is realizable with a bit rate of b_{p_k} bits per symbol. b_{p_k} is chosen from a set $\{b_{p_k}\}_{p_k=1}^P$, $p = 1, 2, \dots, P$ according to the given total energy E_T and the channel conditions. The high speed data stream are demuxed beforehand to K^* and then placed into $(N_U \times 1)$ dimensional vector \underline{u}_k for $k = 1, 2, \dots, K^*$. Then, these data packets are channel encoded to produce $(B \times 1)$ dimensional vector \underline{d}_k . The elements of these \underline{d}_k vectors are then mapped to symbols using quadrature amplitude modulation (QAM) scheme with M constellations. So defining channel encoder rate as $r_{code} = \frac{N_U}{B}$, the realizable discrete rates can be written as $b_p = r_{code} \log_2 M$. If we define N as the spreading sequence length, T_C as chip period and TTI as the transmission time interval for a packet, the number of symbols transmitted in a packet is given by $N^{(x)} = \frac{TTI}{NT_C}$. Then, $(N^{(x)} \times 1)$ dimensional vectors $\underline{x}_k = [x_k(1), \dots, x_k(p), \dots, x_k(N^{(x)})]^T$ are produced from the transmission symbols corresponding to the vectors \underline{d}_k for each $k = 1, 2, \dots, K^*$. So we can consider $(N^{(x)} \times K^*)$ the

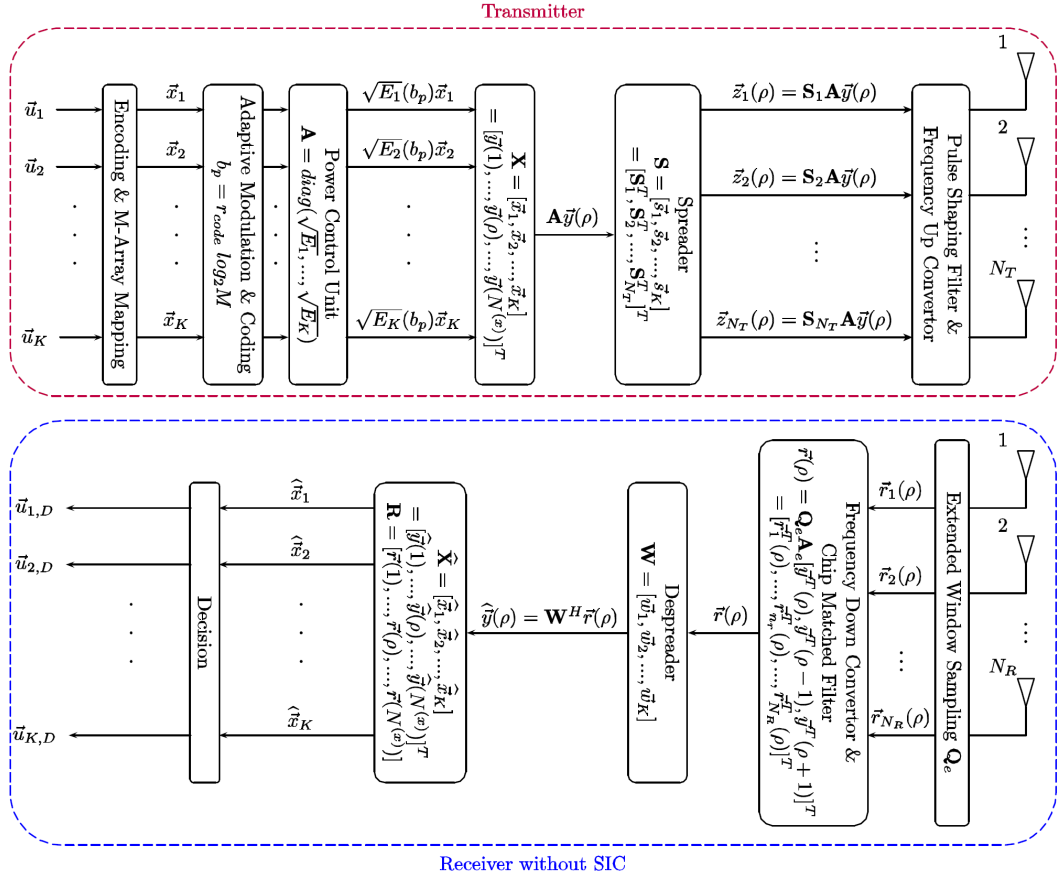


Figure 2.1: Margin Adaptive HSDPA-MIMO System Model

transmitted symbol matrix as

$$\mathbf{X} = [\underline{x}_1, \dots, \underline{x}_k, \dots, \underline{x}_{K^*}] \quad (2.1)$$

For defining the data sent in each symbol period \mathbf{X} can also be written as

$$\mathbf{X} = [\underline{y}(1), \dots, \underline{y}(p), \dots, \underline{y}(N^{(x)})]^T \quad (2.2)$$

where the transmitted vector $\underline{y}(p)$ contains symbols from each channel, which have unit average energy $E(y_k(p)y_k^*(p))=1$, over the symbol period p . For giving different energies to channels, amplitude matrix $A = \text{diag}(\sqrt{E_1}, \dots, \sqrt{E_k}, \dots, \sqrt{E_{K^*}})$ is used. The con-

straint here is total energy is equal to or more than the allocated energies to the channels,

$$E_T \geq \sum_{k=1}^K E_k.$$

The next part after assigning the energies is spreading the symbols using the spreading codes. For this the $(N \times K^*)$ dimensional $\mathbf{S}_{n_t} = [\underline{s}_{n_t,1}, \dots, \underline{s}_{n_t,k}, \dots, \underline{s}_{n_t,K^*}]$ matrices are used which are defined for each transmitter antennas. That's why signature sequence matrix for a MIMO system with N_T antennas is as follows

$$\mathbf{S} = [\mathbf{S}_1^T, \dots, \mathbf{S}_{n_t}^T, \dots, \mathbf{S}_{N_T}^T]^T = [\underline{s}_1, \dots, \underline{s}_{K^*}] \quad (2.3)$$

where $|\underline{s}_k|^2 = 1$. Different channels under a transmitter antenna generates different sequences for a symbol period as it can be understood from the signature sequence matrix. These spreading sequences multiplied with symbols and their amplitudes will be combined in the corresponding transmitter antenna. The combined spreaded symbols vector for the transmitter antenna n_t at a specific symbol period p can be written mathematically as

$$\underline{\mathbf{z}}_{n_t}(p) = [z_{n_t,1}(p), \dots, z_{n_t,N}(p)]^T = \mathbf{S}_{n_t} \mathbf{A} \underline{\mathbf{y}}(p) \quad (2.4)$$

These vectors generated for each transmitter antennas are then pulse shaped with a chip period T_C , up-converted to the desired frequency and sent from their corresponding antennas.

The multipath channel used in the system model is assumed to have L resolvable paths and be constant in TTI. This means coherence time of the channel is longer than the TTI. Between every packet transmission the channel is measured with a pilot and then the transmitter is informed. The channel impulse response for a combination of a transmitter and a receiver antenna can be represented by a vector, $\underline{h}^{(n_r, n_t)} = [h_0^{(n_r, n_t)}, \dots, h_{L-1}^{(n_r, n_t)}]^T$. So its $((N + L - 1) \times N)$ dimensional channel convolutional matrix is

$$\mathbf{H}^{(n_r, n_t)} = \begin{bmatrix} h_0^{(n_r, n_t)} & 0 & 0 \\ \vdots & h_0^{(n_r, n_t)} & \vdots \\ h_0^{(n_r, n_t)} & \vdots & \ddots & 0 \\ 0 & h_0^{(n_r, n_t)} & & h_0^{(n_r, n_t)} \\ \vdots & \vdots & \ddots & \vdots \\ 0 & 0 & & h_0^{(n_r, n_t)} \end{bmatrix} \quad (2.5)$$

This is a channel convolutional matrix for combination given above can be generalized for the whole MIMO system with a $(N_R(N + L - 1) \times NN_T)$ matrix,

$$\mathbf{H}^{(n_r, n_t)} = \begin{bmatrix} \mathbf{H}^{(1,1)} & \dots & \mathbf{H}^{(1, N_T)} \\ \vdots & \ddots & \vdots \\ \mathbf{H}^{(N_r, 1)} & \dots & \mathbf{H}^{(N_r, N_T)} \end{bmatrix} \quad (2.6)$$

The length of the spreaded symbols become longer after transmitted over the multi-path channels. When despreading the signals at the receiver side, the effect of the channel should also be taken into the account. Therefore $(N_R(N + L - 1) \times K^*)$ dimensional receiver matched filter signature sequence matrix is written as

$$\mathbf{Q} = \mathbf{HS} = [\underline{q}_1, \dots, \underline{q}_k, \dots, \underline{q}_{K^*}] \quad (2.7)$$

where the receiver matched filter despreading sequence is represented by a $(N_R(N + L - 1) \times 1)$ dimensional vector, $\underline{q}_k = \mathbf{H}\underline{s}_k$. Having longer sequences make them overlap and losing their orthogonality. As aforementioned in the introduction part, this causes ISI and ICI. So the received spreaded current symbol is affected by the previous and the next symbols. This should be taken into account at the receiver side for handling ISI. Thus in order to express it mathematically, the $(N_R(N + L - 1) \times 3K^*)$ dimensional extended receiver signature sequence matrix is formed

$$\mathbf{Q}_e = [\mathbf{Q}, \mathbf{Q}_1, \mathbf{Q}_2] \quad (2.8)$$

where

$$\mathbf{Q}_1 = [\mathbf{I}_{N_R} \otimes (\mathbf{J}^T)^N] \mathbf{Q} = [\underline{\mathbf{q}}_{1,1}, \dots, \underline{\mathbf{q}}_{K^*,1}] \quad (2.9)$$

$$\mathbf{Q}_2 = [\mathbf{I}_{N_R} \otimes \mathbf{J}^N] \mathbf{Q} = [\underline{\mathbf{q}}_{1,2}, \dots, \underline{\mathbf{q}}_{K^*,2}] \quad (2.10)$$

$\underline{\mathbf{q}}_{k,1}$ and $\underline{\mathbf{q}}_{k,2}$ are the overlapped portions the previous and the next receiver signature sequences with the current one. $(N + L - 1) \times (N + L - 1)$ dimensional \mathbf{J} matrix is used to choose and shift these overlapped regions in the sequences. Above \mathbf{J} is used for $\mathbf{J}_{(N+L-1)}$ for the simplicity in the notation. Mathematically $\mathbf{J}_{(N+L-1)}$ is defined as

$$\mathbf{J}_{(N+L-1)} = \begin{bmatrix} \mathbf{0}_{(N+L-2)} & 0 \\ \mathbf{I}_{(N+L-2)} & \mathbf{0}_{(N+L-2)} \end{bmatrix}.$$

The received signal is first down converted, passed through the receiver chip matched filter and then sampled at the chip period intervals T_C . After this process, the $(N + L - 1) \times 1$ dimensional vector $\underline{r}_{n_r}(p) = [r_{n_r,1}(p), \dots, r_{n_r,(N+L-1)}(p)]^T$ is obtained in each receiver antenna for a symbol period p . The total received signal matrix for the receiver antenna n_r is $\mathbf{R}_{n_r} = [\underline{r}_{n_r}(1), \dots, \underline{r}_{n_r}(p), \dots, \underline{r}_{n_r}(N)]$. For a symbol period p , the received signal vector in all antennas can be written as follows in terms of $\underline{y}(p)$,

$$\underline{r}(p) = [\underline{r}_1^T(p), \dots, \underline{r}_{n_r}^T(p), \dots, \underline{r}_{N_R}^T(p)]^T = \mathbf{Q}_e (\mathbf{I}_3 \otimes \mathbf{A}) \begin{bmatrix} \underline{y}(p) \\ \underline{y}(p-1) \\ \underline{y}(p+1) \end{bmatrix} + \underline{n}(p) \quad (2.11)$$

where $N_R(N + L - 1)$ dimensional zero mean circularly symmetric complex gaussian noise $\underline{n}(p)$ has the correlation matrix $E(\underline{n}(p)\underline{n}^H(p)) = 2\sigma^2\mathbf{I}_{N_R(N+L-1)}$ with one dimensional noise variance $\sigma^2 = \frac{N_0}{2}$. The total received signal matrix that includes all symbols of the packet is given as $\mathbf{R} = [\underline{r}(1), \dots, \underline{r}(N)] = [\mathbf{R}_1^T, \dots, \mathbf{R}_{N_R}^T]^T$.

The receiver uses $\underline{r}(p)$ to estimate the transmitted symbol vector at symbol period p . Linear MMSE equalizer despreading matrix, which is formed from LMMSE despreading

filter coefficients, $\mathbf{W} = [\underline{w}_1, \dots, \underline{w}_k, \dots, \underline{w}_{K^*}]$ is used to perform this estimation.

$$\hat{\underline{y}}(p) = [\hat{y}_1(p), \dots, \hat{y}_k(p), \dots, \hat{y}_{K^*}(p)] = \mathbf{W}^H \underline{r}(p) \quad (2.12)$$

In designing \mathbf{W} , two considerations were taken into account to get the best performance from the equalizer. These are $\underline{w}_k^H \underline{q}_k = 1$ and $\underline{w}_k^H \underline{q}_j$ is minimum for $j \neq k$. \underline{w}_k satisfying these conditions is given as

$$\underline{w}_k = \frac{\mathbf{C}^{-1} \underline{q}_k}{\underline{q}_k^H \mathbf{C}^{-1} \underline{q}_k} \quad (2.13)$$

and

$$\mathbf{C} = \mathbf{Q}_e (\mathbf{I}_3 \otimes \mathbf{A}^2) \mathbf{Q}_e^H + 2\sigma^2 \mathbf{I}_{N_R(N+L-1)} \quad (2.14)$$

where \mathbf{C} is the $N_R(N+L-1) \times N_R(N+L-1)$ dimensional received signal covariance matrix, $\mathbf{C} = E(\underline{r}(p) \underline{r}^H(p))$. Other calculation for the covariance matrix is as follows,

$$\mathbf{C}_k = \mathbf{C}_{k-1} + E_k \underline{q}_k \underline{q}_k^H + E_k \underline{q}_{k,1} \underline{q}_{k,1}^H + E_k \underline{q}_{k,2} \underline{q}_{k,2}^H \quad (2.15)$$

for $k = 0, 1, \dots, K^*$ and $\mathbf{C} = \mathbf{C}_{K^*}$, $\mathbf{C}_0 = 2\sigma^2 \mathbf{I}_{N_R(N+L-1)}$.

The mean-square error at the receiver is written as $\varepsilon_k = E(|\hat{\underline{y}}(p) - \underline{y}(p)|^2)$. The system value of a channel λ_k is given as follows,

$$\lambda_k = 1 - \varepsilon_k = \frac{\gamma_k}{1 + \gamma_k} = E_k \underline{q}_k^H \mathbf{C}^{-1} \underline{q}_k \quad (2.16)$$

where γ_k is the signal to noise ratio (SNR) of the output of each receivers for different channels. We can deduce the following from the famous Shannon's capacity equation

$$\gamma_k = \Gamma \left(2^{b_k} - 1 \right) \quad (2.17)$$

where b_k is the number of bits per symbol for a specific channel.

Since the aim of the work done here is to optimize the total MMSE, $\varepsilon_T = \sum_{k=1}^{K^*} \varepsilon_k$ should be minimized. Alternatively this means maximizing $\lambda_T = \sum_{k=1}^{K^*} \lambda_k$ since $\lambda_k = 1 - \varepsilon_k$ [16].

Combining the 2.16 and 2.17, we get

$$E_k = \frac{\lambda_k^*(b_{p_k})}{\underline{q}_k^H \mathbf{C}^{-1} \underline{q}_k} = \frac{\Gamma(2^{b_{p_k}} - 1)}{(1 + \Gamma(2^{b_{p_k}} - 1)) \underline{q}_k^H \mathbf{C}^{-1} \underline{q}_k} \quad (2.18)$$

2.18 shows us how to calculate E_k for a selected bit rate b_{p_k} from the discrete set. The significance of showing above relations is to demonstrate the fact that both E_k and \mathbf{C} are the functions of each other. Since we are interested in finding E_k , we have to make iterative calculations to solve this problem.

For each discrete bit rate in a set, the iterative energy calculations are carried out until the energy converges to a value. Then it is decided which bit rate to be used by maximizing the total rate while satisfying $E_T \geq \sum_{k=1}^{K^*} E_k$. This is how the energies are optimized and the bit rates are chosen in non-SIC case.

In fact, there is an option to load each E_k with $\frac{E_T}{K^*}$ instead of carrying out iterative calculations; however, this leads to non-discrete bit rates which is impractical. This type of loading is used merely for calculating the upper bound. This is because the λ_T is maximized when $E_k = \frac{E_T}{K^*}$ [16]. For the MMSE receivers with or without SIC, the total system capacity is given as

$$C_T = \sum_{k=1}^{K^*} \log_2 \left(1 + \frac{\lambda_k}{(1 - \lambda_k)\Gamma} \right) \quad (2.19)$$

where Γ is the gap value. The difference of upper bounds of SIC and non-SIC schemes stems from the difference in calculations of the λ_k .

2.0.2 Successive Interference Cancellation Receiver

The system model for SIC receiver is shown in figure (2.2) [24].

The advantages and elegance of the SIC receiver arises from the difference in the

$$\mathbf{R}_{k-1} = \mathbf{R}_k - \sqrt{E_k} \Phi_k \quad (2.21)$$

and

$$\Phi_k = \underline{q}_k \widehat{\mathbf{x}}_k^T + \underline{q}_{k,1} (\mathbf{J}_{N(x)} \widehat{\mathbf{x}}_k)^T + \underline{q}_{k,1} (\mathbf{J}_{N(x)}^T \widehat{\mathbf{x}}_k)^T \quad (2.22)$$

Here $\mathbf{J}_{N(x)}$ and $\mathbf{J}_{N(x)}^T$ are used to specify the previous and the next received ISI symbols. The received despread signal vector is computed as $\widehat{\mathbf{x}}_k^T = \underline{w}_k^H \mathbf{R}_k$.

In order to get the best performance in SIC, the system values, $\lambda_k = E_k \underline{q}_k^H \mathbf{C}_k^{-1} \underline{q}_k$, are ordered in an ascending order. Therefore, the symbols in the strongest channel, which means less affected from the others, are detected first and the system operates with using this highly reliable information. As eliminating the effects from other channels, originally weak channels at the end of the detection process become stronger with SIC scheme.

How SIC works has been explained up to here. This part of the report concentrates on calculation of \mathbf{C}_k and E_k in SIC. It is proven in [16] with matrix inversion lemma that \mathbf{C}_k can be calculated as follows,

$$\begin{aligned} \mathbf{C}_k^{-1} &= \mathbf{C}_{k-1}^{-1} - \zeta \underline{d} \underline{d}^H - (\zeta_1 + \zeta \zeta_1^2 |\xi_3|^2) \underline{d}_1 \underline{d}_1^H \\ &\quad - (\zeta_2 + \zeta \zeta_2^2 |\xi_4|^2) \underline{d}_2 \underline{d}_2^H \\ &\quad + \zeta \zeta_1 (\xi_3 \underline{d} \underline{d}_1^H + \xi_3^* (\underline{d} \underline{d}_1^H)^H) + \zeta \zeta_2 (\xi_4 \underline{d} \underline{d}_2^H + \xi_4^* (\underline{d} \underline{d}_2^H)^H) \\ &\quad - \zeta \zeta_1 \zeta_2 (\xi_3 \xi_4^* \underline{d}_2 \underline{d}_1^H + (\xi_3 \xi_4^*)^* (\underline{d}_2 \underline{d}_1^H)^H) \end{aligned} \quad (2.23)$$

where distance vectors are computed as

$$\underline{d} = \mathbf{C}_{k-1}^{-1} \underline{q}_k, \quad \underline{d}_1 = \mathbf{C}_{k-1}^{-1} \underline{q}_{k,1}, \quad \underline{d}_2 = \mathbf{C}_{k-1}^{-1} \underline{q}_{k,2} \quad (2.24)$$

and weights are

$$\xi = \underline{d}^H \underline{q}_k, \xi_1 = \underline{d}_1^H \underline{q}_{k,1}, \xi_2 = \underline{d}_2^H \underline{q}_{k,2}, \xi_3 = \underline{d}^H \underline{q}_{k,1}, \xi_4 = \underline{d}^H \underline{q}_{k,2} \quad (2.25)$$

$$\zeta = \frac{E_k}{1 + \Gamma(2^{b_{pk}} - 1)}, \zeta_1 = \frac{E_k}{1 + E_k \xi_1}, \zeta_2 = \frac{E_k}{1 + E_k \xi_2} \quad (2.26)$$

It is important to note that \mathbf{C}_k^{-1} depends on \mathbf{C}_{k-1}^{-1} without any matrix inversions. Iterative energy calculation $E_{k,i}$ can be simplified to

$$E_{k,i} = \frac{\gamma_k^*}{\xi - E_{k,(i-1)} \left(\frac{|\xi_3|^2}{1 + E_{k,(i-1)} \xi_1} + \frac{|\xi_4|^2}{1 + E_{k,(i-1)} \xi_2} \right)} \quad (2.27)$$

2.0.3 System Value Approach for Determining Rates

To find the maximum discrete rate b_p that maximizes $R_T = K^* b_p$ and satisfies $E_T \geq \sum_{k=1}^{K^*} E_k$, energies are calculated in non-SIC and SIC cases for every element of the discrete bit rate set with using $\lambda_k^*(b_p)$ as shown in (2.18). However, the bit rate that maximize the system throughput can be found without energy allocation as follows

$$\lambda_k^*(b_p) \leq \lambda_{mean} \leq \lambda_k^*(b_{p+1}) \quad (2.28)$$

where $\lambda_{mean} = \frac{1}{K^*} \sum_{k=1}^{K^*} \lambda_k$ and taking $E_k = \frac{E_T}{K^*}$. This eases the computation since the iterative calculations are just done for the found bit rate, not for the whole discrete set.

2.0.4 Two-Group Approach

Further optimization in system throughput can be achieved with two group approach. As shown in (2.28) the λ_{mean} must be higher than $\lambda_k^*(b_{p+1})$ for the total throughput be $R_T = K^* b_{p+1}$. Even λ_{mean} is slightly less than $\lambda_k^*(b_{p+1})$, the total rate is still $R_T = K^* b_p$. Therefore, the energy difference $E_T - \sum_{k=1}^{K^*} E_k$, which is called residual energy, cannot be used for increasing the total throughput. With two group approach this residual energy is decreased by loading higher bit rates to some channels. Thus, two discrete bit rates are used in two group approach. b_p, b_{p+1} and the number of channels m that carries b_{p+1} can

be found with the following

$$(K^* - m)\lambda_k^*(b_p) + m\lambda_k^*(b_{p+1}) \leq \lambda_{mean} \leq (K^* - m - 1)\lambda_k^*(b_p) + (m + 1)\lambda_k^*(b_{p+1}) \quad (2.29)$$

It is noted that the range between the inequalities is diminished now.

Chapter 3

Capacity Simulations

3.1 Background

FOR measuring the performances of SIC and the non-SIC cases and comparing them with upper bound, a simulation has been done. The parameters used in the simulation are followings: the total number spreading sequences is $K = 32$, the number of used channels is $K^* = 30$, the spreading factor is $N = 16$, transmitter and receiver antenna number is $Nt = Nr = 2$, and the additive white noise variance is $\sigma^2 = 0.02$. The bit rate per symbol set is from 0 to 6 with 0.25 bit granularity. The gap value is $\Gamma = 0$ dB. Channels are generated from the following square root power delay profiles (PDP): $\underline{h}_{veh_A} = [0.7478, 0.594, 0.2623, 0.133]$, $\underline{h}_{ped_A} = [0.9923, 0.1034, 0.0683]$ and $\underline{h}_{ped_B} = [0.6369, 0.5742, 0.3623, 0, 0.253, 0, 0, 0, 0.2595]$. These square root PDPs represent different scenarios that are likely in mobile communications. From each of above square root PDPs 30 different channel impulse responses are generated randomly to average the effects of the channel. The spreading sequences are determined from the eigenvectors of $G = H^H H$ which have the highest 30 eigenvalues. The sequences are further ordered according to their eigenvalues. This method is explained in [13]. The capacities are recorded for given SNR values from 0 to 40 dB. Channels are normalized to 1 so these SNR values correspond to $\frac{E_T}{N_0}$.

Throughputs of different allocation schemes, namely margin adaptive constrained

optimization, two- group constrained optimization, SIC constrained optimization, SIC two group constrained optimization are simulated. Besides, gaussian upper bound, margin adaptive upper bound and SIC upper bound are drawn in order to compare the results. The gaussian upper bound is obtained by making $L=1$ and equating its single PDP element to 1. Then for all upper bounds are obtained using the equation (2.19). The only difference is that $\lambda_k = E_k \underline{q}_k^H \mathbf{C}^{-1} \underline{q}_k$ is used for non-SIC scheme whilst $\lambda_k = E_k \underline{q}_k^H \mathbf{C}_k^{-1} \underline{q}_k$ is used for the SIC. Since \mathbf{C} is computed iteratively by adding all \mathbf{C}_k matrices (2.15), frobenius norm of \mathbf{C} is larger than frobenius norm of \mathbf{C}_k . Similarly, frobenius norm of \mathbf{C}^{-1} is smaller than the frobenius norm of \mathbf{C}_k^{-1} . This yields smaller system value in non-SIC case. In energy calculation (2.18), the term $\underline{q}_k^H \mathbf{C}_k^{-1} \underline{q}_k$ is in denominator, so it results in less required energy for same bit rate in SIC scheme.

For the margin adaptive loading the energies are found iteratively for the all bit rates in the set. After the finding all E_k values for an iteration, \mathbf{C} is updated. Then \mathbf{C} is inverted to get \mathbf{C}^{-1} which is needed for the energy calculation. With new \mathbf{C}^{-1} value, the energies are calculated again in the next iteration. It is checked if the energy value for a channel converges to a single value in each iteration. By convergence, the simulation takes $E_{k,i} - E_{k,(i-1)} < 0.001 E_{k,(i-1)}$ as a reference. If this convergence cannot be reached, the iterative calculations are performed until the 100th time. It is seen that checking the convergence increases the timing performance of the simulation significantly. After finding the converged E_k values, $E_T \geq \sum_{k=1}^{K^*} E_k$ condition, which is the constraint in the optimization, is checked. If this condition still holds true, the calculations are done for the next bit rate in the set. Thus, the maximum bit rate b_p that satisfy the constrained is found. The system throughput is $R_T = K^* b_p$ in the margin adaptive case.

For the SIC scheme, the bit rate that will be used is found with the system value approach. Then the energies are allocated with the equation (2.27). There is no need to update \mathbf{C}_k , in each iteration since calculation of E_k is a function of \mathbf{C}_{k-1} not \mathbf{C}_k . This decreases the computation time significantly. Furthermore, there is no matrix inversions even in the calculation of the \mathbf{C}_k . There is only one matrix inversions in this scheme which one is needed for determining the bit rate in system value approach. SIC is superior

compared to the margin adaptive loading not only for the system throughput point of view but also for the computation time.

Loading with two group for the margin adaptive and SIC cases are quite similar to each other. First the bit b_p , which is used in the transmission, is found with the margin adaptive or SIC calculations explained above. Then the iterations are done for each possible m value until finding the maximum m satisfying $E_T \geq \sum_{k=1}^{K^*} E_k$. The total capacity is $R_T = (K^* - m)b_p + mb_{p+1}$ in this allocation way. However, this scheme also increases the computation time since further iterations are needed for determining m .

The Pedestrian A channel has 3 taps which the first one is very strong and the others are weak. This is the case where most of the energy comes from the line of sight element. Since it is still a multipath channel, the inter-symbol interference occurs. However, the effects of ISI are not as influential as the other channels because the number of taps is relatively less and the second and third taps are weak. That's why the upper bounds for SIC and non-SIC allocations are closer to the Gaussian upper bound which has only one tap compared to the other channels.

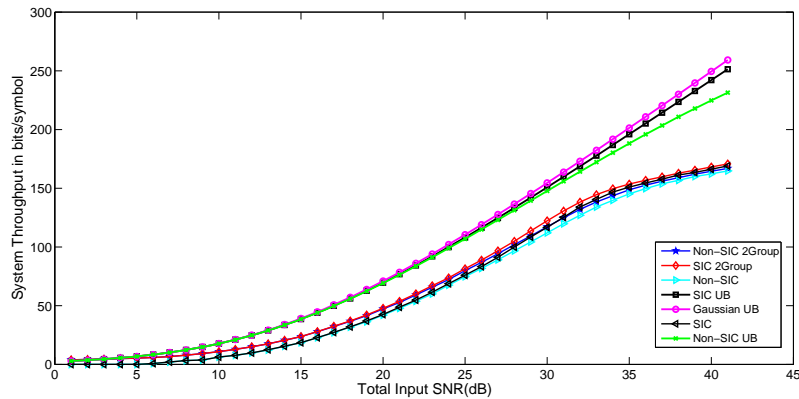


Figure 3.1: Pedestrian A Channel Results

The Pedestrian B channel has 9 delay bins and the variances of the energies in the multipath components are relatively balanced. This channel is the worst channel with regard to ISI. Hence, this is the type of a channel where SIC shows its advantage most. From the simulation results we observe that the constrained optimization results are very

close even to the Gaussian Upper Bound. In most input SNR values there is only 3 dB difference and in some input SNRs even lower than that for the 2-group allocation. In addition, the margin adaptive allocation gives us so low capacity that the difference between it and SIC is outstanding.

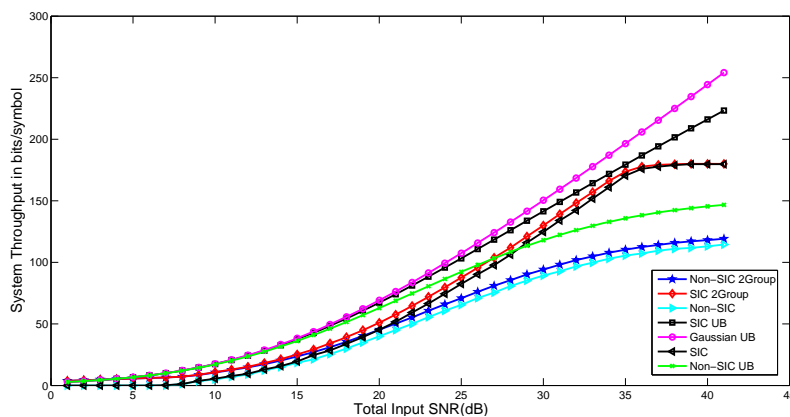


Figure 3.2: Pedestrian B Channel Results

The vehicular A channel is at somewhere between the other channels in terms of the ISI effect and efficiency of the SIC receiver. SIC increases the capacity substantially for this case too.

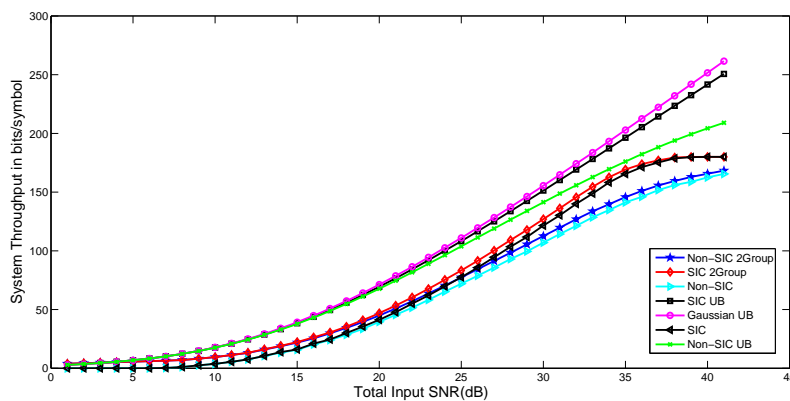


Figure 3.3: Vehicular A Channel Results

Chapter 4

End to End Transmission Simulations

4.1 Simulation Setup

IN capacity simulations, the rates were simulated according to the energy allocation results. With the total available energy, different allocation schemes were compared from the total rate maximization point of view. However, the system model presented in figure 2.1 and figure 2.2 have not been simulated. For observing the operation of the allocation schemes as a total system and if the expected results are got, these simulations were needed and done.

The main objective of the end to end transmissions is to allocate the given energy according to the scheme which is desired to be simulated and receive signal to interference plus noise ratio per channel. With these received SNIR values, one can easily find how many bits per symbol a channel allows to transmit with the given error probability. The relation between bit rates and the error probability is determined by the Gap value. In end to end transmissions, it is normally expected to get the capacity values that are simulated and got from the previous simulations for the same set of parameters.

As initial configuration of the parameters the set of parameters used in capacity calculations are used for obtaining consistency among the simulations and comparing

them. Therefore the total number spreading sequences is again $K = 32$, the number of used channels is $K^* = 30$, the spreading factor is $N = 16$, transmitter and receiver antenna number is $Nt = Nr = 2$, and the additive white noise variance is 0.02. The bit rate per symbol set is from 0 to 6 with 0.25 bit granularity. The gap value is $\Gamma = 0dB$. Channels are generated from the following square root power delay profiles (PDP): $\underline{h}_{veh_A} = [0.7478, 0.594, 0.2623, 0.133]$, $\underline{h}_{ped_A} = [0.9923, 0.1034, 0.0683]$ and $\underline{h}_{ped_B} = [0.6369, 0.5742, 0, 0.3623, 0, 0.253, 0, 0, 0, 0.2595, 0, 0, 0, 0, 0.047]$. 20 channels are generated for averaging the results from the given power delay profiles. Since end to end transmission actually creates random data and transmits these with the different algorithms through the system model, these simulations take much more time compared to the capacity simulations. That's why 20 channels rather than 30 were generated. It has been observed that this number is already sufficient for getting smooth curves.

For margin adaptive case, the end to end simulation starts with random generation of the bits. The number of bits generated is quite important here, as it will be explained later more bits gives more consistent and accurate results. Then those bits are mapped to the 4-QAM symbols. In the system model there are adjustable quadrature amplitude modulators; however, having only 4-QAM is sufficient to measure received SNIRs since as it will be described later, the actual inputs are used for measuring SNIR. Since the decision has not been done the received SNIR values are independent of the fact which QAM has been used.

The channel convolution matrix is formed at the beginning of the simulation just like in the capacity simulations. Afterwards the strong signature sequences are chosen as discussed in the capacity simulations section. Later the function which makes energy allocation for the capacity calculations is used. This function takes Qe , Et , K , b_{pk} , No and Γ as inputs and outputs the allocated energies and the expected capacity according to these parameters. The operation of this function is discussed in the capacity simulations section.

In capacity simulation, the allocated energies are determined just to check if the sum of them exceeds total available energy. Since there was no transmission in that kind

of simulations, there was no place to use individual energies per channels information. Whereas, the symbols in each channels are multiplied with the amplitudes, which are square roots of the energies per channel, in the end to end simulation.

Then the received signal matrix \mathbf{R} is formed in the simulation. As it is known the frequency selective channels have more than one tap and the symbols are spread into subsequent symbols if they pass through this kind of channel. This effect has to be reflected to the simulation. Assume that the signal at symbol time ρ is being tried to be set in the receiver side. The signal at symbol time ρ contains the portions of from symbols of $\rho - 1$ and $\rho + 1$ times. The tail of the symbol at $(\rho - 1)$ overlaps with the head of the symbol at ρ . Similarly, the head of the symbol at time $(\rho + 1)$ overlaps with the tail of the symbol at ρ . In the formula (2.11), received signal matrix at symbol time ρ is found by taking this effect into account.

After the formation of the received signal, the equalizer matrix is generated by using the formula (2.13). In margin adaptive case, the C^{-1} is directly calculated from the C by taking inverse of it. Once the LMMSE equalizer receiver matrix is generated, the received symbols can be found by multiplying the hermitian of the equalizer matrix with the received signal matrix. Afterwards, the received signal to noise and interference ratios per channel can be calculated since we know the received. The SNIR values are calculated by the formula:

$$SNIR_k = \frac{E_k \underline{x}_k^T (\underline{x}_k^T)^H}{(\hat{\underline{x}}_k - \sqrt{E_k} \underline{x}_{k,D}) (\hat{\underline{x}}_k - \sqrt{E_k} \underline{x}_{k,D})^H} \quad (4.1)$$

and $\hat{\underline{x}}_k = \underline{w}_k^H \mathbf{R}$. Note that \underline{x}_k is a column vector. $\underline{x}_{k,D}$ is decided symbols after the reception. However in the end to end transmission simulations, channel encoder has not been integrated to the system, therefore instead of the decided symbols the original symbols are used in the calculation of SNIR per channels. This is needed to calculate the values correctly.

After getting the values, the capacity per channel is calculated with the well known

following formula:

$$b_{pk} = \log_2\left(1 + \frac{SNIR_k}{\Gamma}\right) \quad (4.2)$$

When one group allocation is used, the total capacity is found by the multiplying the number of channels with the minimum of the values. Minimum value out of the channel capacities is chosen since in one group all channels should satisfy the determined bit rate. So total capacity for end to end transmission simulation is the following.

$$C = K^* \min(b_{pk}) \quad (4.3)$$

SIC end to end transmission simulation setup is quite similar with the margin adaptive with a couple of differences. The main difference is in the energy allocation function, as it makes sense. The responsible function from the energy allocation to the channels was written for the capacity calculation simulations before. However since this kind of simulation is interested only in the energy allocation and the comparison of E_T with the $\sum_{k=1}^{K^*} E_k$, it used not to output \mathbf{C}_k^{-1} which is essential in the MMSE linear equalizer despreading filter coefficients \underline{w}_k calculations. MMSE filter coefficients are calculated in SIC with the equation (2.20). As aforementioned, the SIC formulation given in the **system model part of** the report has approximations in order to decrease the computation complexity. Approximations are used in the calculation of the \mathbf{C}_k^{-1} matrices. When allocating the energies these approximated values are found and used. Once energies are allocated \mathbf{C}_k^{-1} values can be found by equation (2.23), yet it means matrix inversion for each channel. Since those matrices are already calculated inside of the energy allocation function there is a need to output these matrices together with allocated energies. In MATLAB, this problem is solved by storing the values in a 3-dimensional matrix whose 3rd dimension is different channels. Then, this matrix is outputted.

After the energies are allocated and the covariance matrices are found, MMSE linear equalizer despreading filter coefficients are calculated. Afterwards, the received signal matrix \mathbf{R} is found with running same algorithm for margin adaptive case. The operation of this part is explained before. However the output of this algorithm gives us \mathbf{R}_{K^*} . By

using formula (2.21), the received signal matrices for different channels are calculated. This feedback algorithm is the main difference of the SIC receiver. In this way, the effects of channels to the other ones due to the loss of orthogonality are removed one by one. The latest channel of the process is the clearest channel since effects of all other channels are removed. In the process, the rest is to calculate received $SNIR_k$ values with equation (4.1) and find the achievable capacity with those values.

4.2 Results

4.2.1 Margin Adaptive Allocation Scheme

First the end to end simulation was run by sending 100 bits. Since this kind of simulation takes more time compared to the previous simulations, it was firstly thought that decreasing number of bits used in simulations is a beneficial for obtaining the results faster. However, as it can be seen in below figure the results were not the expected ones in this case.

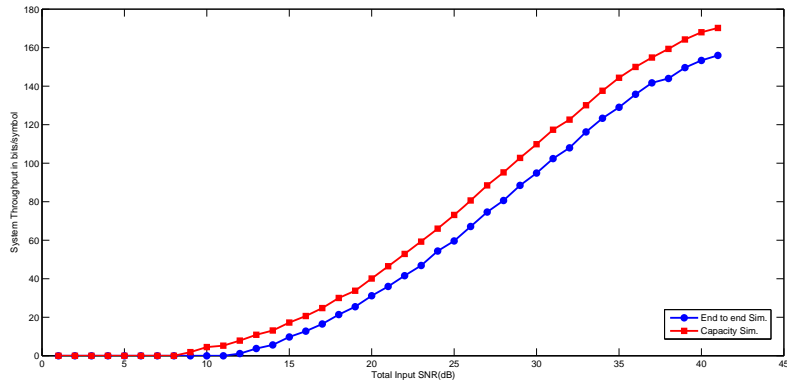


Figure 4.1: Margin Adaptive-Vehicular A-100 bits

As aforementioned, the two curves represent the capacity simulation results and the end to end simulation results of margin adaptive allocation scheme. Capacity simulations calculates and determines the bit rates according to the total available energy. The end to end simulations determines the bit rates according to the received SNIR values of the channels. Two results were expected to be same; however, there is 15 bits per symbol

difference in nearly every input SNR values. Since bit granularity is 0.25 and there are 30 channels, this means end to end transmission can only satisfy b_{p^*-2} bits/symbol per channel, whereas b_{p^*} bits/symbol per channel should be achievable according to the capacity simulations.

As shown previously, $\mathbf{C} = E\{\underline{r}(\rho)\underline{r}^H(\rho)\}$. This covariance matrix is calculated by the equation (2.14), $\mathbf{C} = \mathbf{Q}_e(I_3 \otimes A^2)\mathbf{Q}_e^H + 2\sigma^2\mathbf{I}_{N_R(N+L-1)}$. This equation holds only when transmitted vectors at different symbol times are uncorrelated, $E\{\underline{y}(\rho)\underline{y}^H(\rho-1)\} = 0$. That is to say, the symbols are assumed to be uncorrelated in the equation (2.14). To satisfy this condition and independent noise addition, the sequence of symbols used in the transmission must be sufficiently long. Taking the actual 3GPP standards into account, the transmission length has been revised to 500 symbols, which is equal to 1000 bits in the used 4-QAM scheme. As it can be observed from the following plot, the results became closer to the previous simulation results.

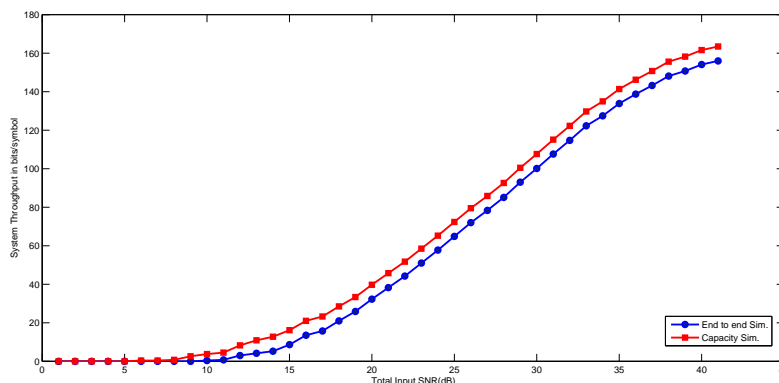


Figure 4.2: Margin Adaptive-Vehicular A-1000 bits

Since the correlation of symbols at different times are closer to zero with this number of transmitted symbols, received SNIR values per channels are more stable around the desired SNIR value. This phenomenon is shown in the following table.

	Desired SNIR per channel	Received mean SNIR	Max. Difference
100 Symbols	18 dB	18.38 dB	1.11 dB
1000 Symbols	18 dB	17.95 dB	0.36 dB

After one group energy allocation, different energies yield same SNR value in all

channels. This is true for both margin adaptive and SIC schemes. This value is called here as desired SNIR per channel. It can be calculated from system values, $SNR_k = \frac{\lambda_k}{1-\lambda_k}$. As it is obvious in the table, the difference amongst the received SNIR per channel values decreases when the number of transmitted symbols is increased. So the variance is diminished together with closer mean to the desired value.

Although the gap between the curves in the above plot is not as much as the previous plot, there is still 7.5 bits per symbol throughput difference. Even the smallest negative variation from the desired SNIR makes this channel transmit with the one lower bit rate in the set. Since only one bit rate is used in all channels, the other channels should use this bit rate as well. So the difference arises from the number of channel and bit granularity multiplication, $7.5 = 30 * 0.25$. The reason and solution of this problem will be discussed later.

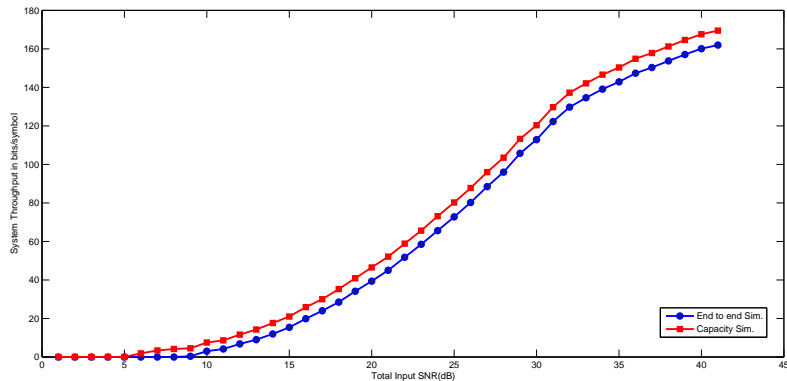


Figure 4.3: Margin Adaptive-Pedestrian A-1000 bits

End to end simulations in pedestrian A and B type of channel also give the same results with 7.5 bits/symbol difference. Since pedestrian A type channel contains less number of delay taps, it gives higher throughput. Due to the interference caused by the long delayed channel, the capacity is low in the pedestrian B channel. In addition, the curves of pedestrian B channel is not as smooth as the other channels.

The contributions of SIC to the capacity was shown in the capacity simulations sec-

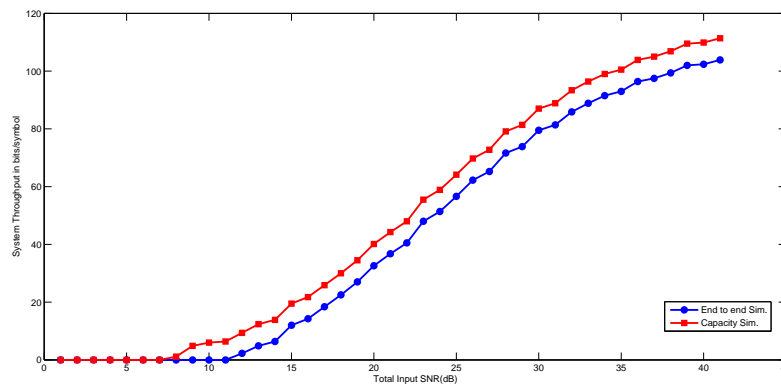


Figure 4.4: Margin Adaptive-Pedestrian B-1000 bits

tion. The other benefit of using SIC is to decrease the computational complexity as explained before. This fact was experienced in the end to end simulations. End to end simulation of margin adaptive scheme in pedestrian B type of channel is the simulation which takes longest time. In order to get smoother curves, the number of channels generated from the power delay profile should be increased; however, this cannot be done because of the excessive operation time of the simulation.

4.2.2 SIC Allocation Scheme

It has been seen in the capacity calculations that SIC allocation scheme provides higher system throughput compared to the margin adaptive energy loading. End to end transmission simulation results have been done to confirm there is not any problem when this type of allocation is used as a system model. In vehicular A and Pedestrian B type of channels, the expected results were obtained except the 7.5 bits/symbol throughput gap. The small variation in the received channel signal to noise ratios occur in the SIC allocation as well. The following plots illustrate simulation results of these channel types.

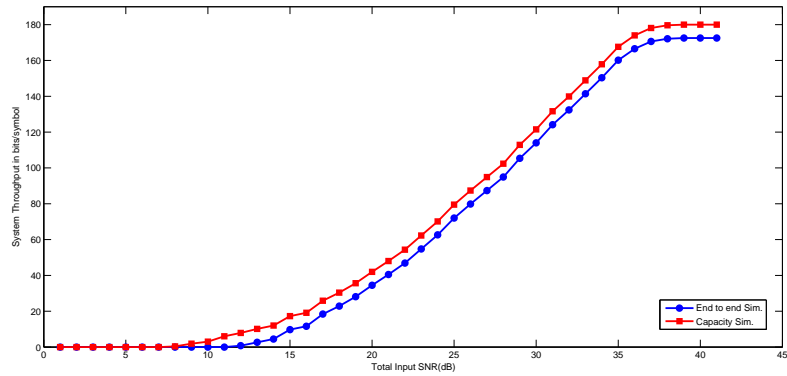


Figure 4.5: SIC-Vehicular A-1000 bits

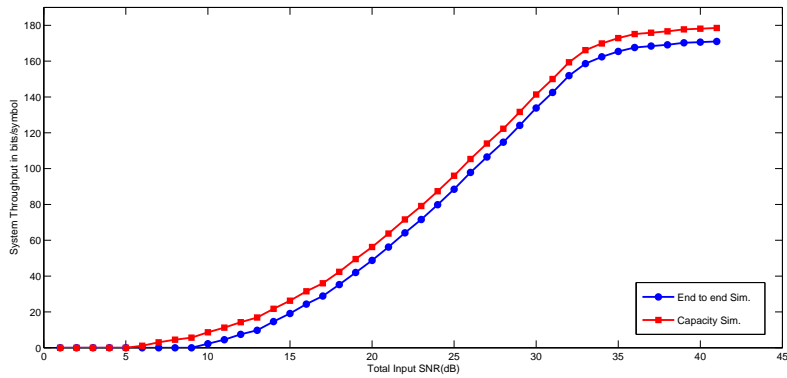


Figure 4.6: SIC-Pedestrian A-1000 bits

Both channels are relatively short and SIC scheme outperforms margin adaptive in terms of capacity and computation complexity as discussed in capacity simulations section. However as channel gets worse, the superiority of SIC to the margin adaptive allocation becomes more dominant. Therefore pedestrian B type of channel is the one where the difference between SIC and margin adaptive allocation system throughputs is the highest. The end to end simulation results together with capacity simulation results for pedestrian B channel in successive interference cancellation system model is presented below.

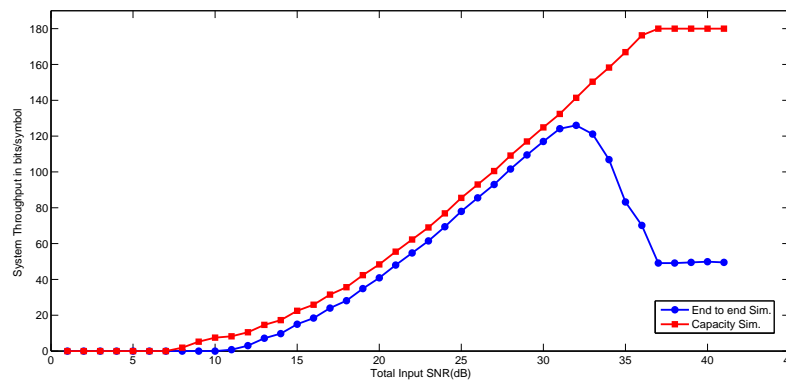


Figure 4.7: SIC-Pedestrian B-1000 bits

Unlike the previous type of channels and margin adaptive allocation scheme, SIC obviously has some problems in the transmission simulations. At low input SNR values, the end to end simulation results are compliant with the capacity simulation results as expected; however, at high input SNR values the end to end simulation results stop following capacity simulation results.

4.2.3 Allocation of the Residual Energy

It has been seen in all end to end simulation results that there is a gap of 7.5 bits/symbol with the capacity simulation results. This means that channels at end to end simulations can transmit with lower bit rate compared to capacity simulations. Since the bit granularity is 0.25 and there are 30 channels, received SNIR of the channels in end to end simulations bear b_{p-1} whereas capacity simulations transmit with b_p . Aforementioned this is caused because of the small variations in the received SNIR values.

Either using system values for determining bit rates or using constraint optimization, the exact SNR that is enough for transmitting b_p is calculated by using the following formula

$$\gamma_k = \Gamma(2^{b_k} - 1) \quad (4.4)$$

which is deduced from Shannon's capacity formula. The energies have been allocated to the channels in a way that they are supposed to provide γ_k received signal to noise ratio values. However, it is seen that the received SNIR values are slightly different than each other. The maximum variation from the mean is around 0.3 dB if a long sequence of symbols is used.

Consider the case when the energies for sending 4.25 bits/symbol per channel are intended to be calculated. According to formula (4.4) with the gap value $\Gamma = 1$, 18 dB of received SNIR value is needed for all channels in one group allocation which can transmit 4.25 bits/symbol in all channels. What is seen after the end to end simulation is that the range of SNIR values between 17.7 dB and 18.3 dB. Since one group allocation is used and all channels must have 18 dB received SNIR value for transmitting 4.25 bits/symbol, only 4 bits/symbol can be transmitted in each channel. Hence the capacity simulation claims that the total throughput is $4.25 * 30 = 127.5$; however, the end to end simulation results give $4 * 30 = 120$. This is where 7.5 bits/symbol difference between two simulations arise.

For equalization purpose, linear minimum mean square error equalizers are used as explained in the introduction section. Although this type of equalizer is not optimal, unlike maximum a posteriori sequence estimators; it is cost effective and practical. The non-optimal equalizer and small correlation between symbols at different times, which can be diminished by sending longer sequence, cause these small variations in the received SNIR values. Increasing the number of bits in the packet diminishes this variation; however, the problem still exists in this case since all received channel SNIR values should be more or equal to the planned value which is calculated by the equation formula (4.4). Yet, after end to end simulation some channel SNIR values are larger and the others are smaller than this value.

One benefit of designing and running end to end simulations is to realize these variations. It is seen that the energies can be allocated taking these received SNIR variations into account. Some margin could be added to channel energies on top of the calculated values. In the system described until this point, the energies are allocated for different

bit rates and then the total allocated energy is checked if it is still smaller than the total available energy. Bit rate is increased and energies are allocated again in case the needed total energy for the previous bit rate is smaller than the total available energy. This process continues until the total available energy is exceeded. Then it is decided that one previous bit rate will be used in the system. Therefore, there is always some amount of unused energy in the system, which is equal to $E_T - \sum_{k=1}^{K^*} E_k$. Aforementioned this energy is called residual energy and how this energy is used in two-group approach in order to increase capacity was explained. Here since one group allocation was used in end to end simulations, this energy can be used as margins for robustness to the variations.

Firstly this residual energy was divided equally and added on top of the allocated energy values in the channels. This can be showed mathematically as $E_k = E_k + \frac{E_T - \sum_{k=1}^{K^*} E_k}{K^*}$. However simulation results showed that this revision worsened the system throughput. It was later realized that adding same amount of energy to the all channels impairs the ratio of allocated energies, which are found with iterative calculations. The result was much worse than the case before allocating the residual energy.

Later the residual energy was allocated in a way that the ratios of the energies found by iterative calculations are preserved. In this way the new energies are found according to the following formula.

$$E_k = E_k + E_k \left(\frac{E_T - \sum_{k=1}^{K^*} E_k}{\sum_{k=1}^{K^*} E_k} \right) \quad (4.5)$$

With this formula, residual energy is allocated to the channels in a way that channels with higher energies get comparatively higher margin than the ones with lower energies. Since same signal to noise ratio is aimed for all channels to have equal bit rates in one group allocation, the relatively worse channels have higher energies and larger portion from the residual energy. The plots below indicate the end to end simulation results with this type of allocation.

In the figure (4.8) the end to end simulation results with SIC scheme in pedestrian B

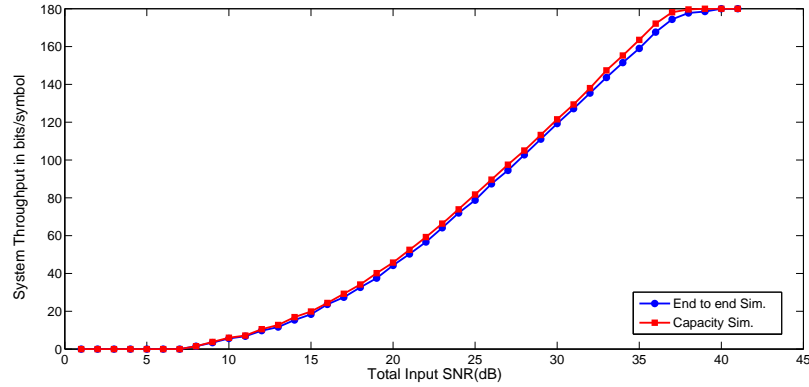


Figure 4.8: Modified SIC with Residual Allocation-Pedestrian B-1000 bits

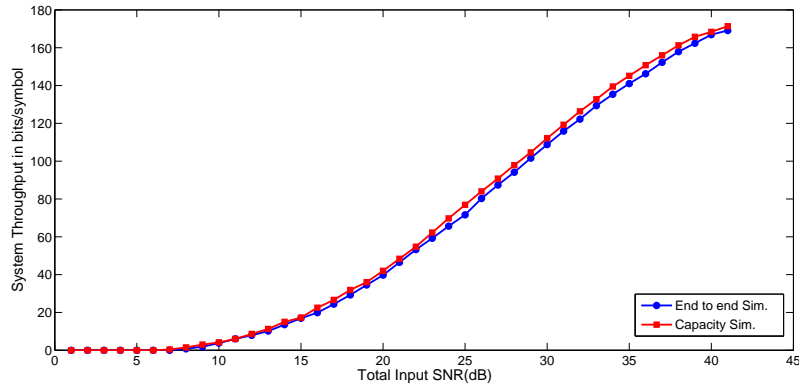


Figure 4.9: Margin Adaptive with Residual Allocation-Vehicular A-1000 bits

type of channel is shown. The gap between two simulations has been nearly disappeared after the distribution of residual energy. There is still some much smaller difference. This is caused by the fact that some received SNIR value is still lower than the planned value despite the margin in some generated channels from the defined power delay profiles. This shows that the quality of the channel also effect the variance of the received SNIR values. In the simulations 20 channels are generated from power delay profiles for averaging the results and in only few of them end to end simulation transmit with b_{p-1} whereas capacity simulations transmit with b_p . Before distributing the residual energy, this was the case in all generated channels. The figure (4.9) shows the results for the margin adaptive allocation in vehicular A type of channel. Allocating unused energy as in the equation (4.5) closes the gap between two simulation types in all types of channels and both allocation schemes.

Chapter 5

Conclusion

This paper shows and compares different throughput allocation schemes in HSDPA MIMO systems. Margin Adaptive allocation and SIC scheme are compared with one group and two group bit loading. Both schemes use linear MMSE for handling intersymbol interference caused by the multipath channel. Unlike the current HSDPA standard, proposed systems in this paper do not apply same energy to the channels. Energies for each channel are computed iteratively by using the covariance matrix. Since channel qualities are quite different, trying to transmit same bit rate with applying same energies to the channels yields inefficiency. In such a case, the total throughput is determined by the worst channel.

The algorithms have been tested by capacity and end to end simulations and needed mathematical revisions and further optimizations were done accordingly. The outcomes with the work explained in this paper are summarized below.

- Higher system throughput (Two-Group, SIC compared to Margin Adaptive)
- Less matrix inversions (SIC)
- Calculating bit rate before the energies (System value approach)

Although margin adaptive allocation is an optimization for the current system, SIC provides much better energy utilization within less operation time. The simulation results justify the foreseen enhancements in the system throughput.

Bibliography

- [1] I. Forkel, H. Klenner, and A. Kemper, “High speed downlink packet access (hsdpa) - enhanced,” *Computer Networks*, vol. 49, pp. 325–340, 2005.
- [2] H. Holma and A. Toskala, *WCDMA for UMTS-HSPA evolution and LTE*, 4th ed. John Wiley, 2007.
- [3] M. Cvitkovic, B. Modlic, and G. Sisul, “High speed downlink packet access principles,” in *IEEE ELMAR 49th International Symposium on on Mobile Multimedia*, 2007, pp. 125–128.
- [4] H. Holma, A. Toskala, K. Ranta-aho, and J. Pirskanen, “High-speed packet access evolution in 3gpp release 7,” *IEEE Commun. Mag. [Online]*, vol. 45, no. 12, pp. 29–35, 2007. [Online]. Available: <http://ieeexplore.ieee.org/stamp/stamp.jsp?arnumber=4395362>
- [5] J. Kim, H. Kim, C. Park, and K. Lee, “On the performance of multiuser mimo systems in wcdma/hsdpa: beamforming, feedback and user diversity,” *IEICE Trans. Commun. (Inst. Electron. Inf. Commun. Eng.)*, vol. 89, no. 8, pp. 2161–2169, 2006.
- [6] K. Freudenthaler, F. Kaltenberger, S. Geirhofer, S. Paul, J. Berkmann, J. Wehinger, C. Mecklenbrauker, and A. Springe, “Throughput analysis for a umts high speed downlink packet access lmmse equalizer,” in *IST 2005*, 2012. [Online]. Available: <http://www.eurasip.org/Proceedings/Ext/IST05/papers/469.pdf>
- [7] C. Mehlfuhrer, S. Caban, , and M. Rupp, “Hsdpa/hsupa handbook.” Chichester: CRC Press, 2010, ch. MIMO HSDPA throughput measurement results, pp. 357–377.

- [8] C. Mehlfuhrer, S. Caban, and M. Rupp, "Measurement-based performance evaluation of mimo hsdpa," *IEEE Transactions on Vehicular Technology*, vol. 59, no. 9, pp. 4354–4367, 2010.
- [9] R. Kwan, M. Aydin, C. Leung, and J. Zhang, "Multiuser scheduling in high speed downlink packet access," *IET Communications*, vol. 3, no. 8, pp. 1363–1370, 2009.
- [10] C.D'Amours and A.O.Dahmane, "Spreading code assignment strategies for mimo-cdma systems operating in frequency-selective channels," *EURASIP Journal on Wireless Communications and Networking*, vol. 2009, pp. 53:1–53:9, 2009. [Online]. Available: <http://dx.doi.org/10.1155/2009/839424>
- [11] K. Alishahi, F. Marvasti, V. Aref, and P. Pad, "Bounds on the sum capacity of synchronous binary cdma channels," *IEEE Transactions on Information Theory*, vol. 55, no. 8, pp. 3577–3593, 2009.
- [12] J. Concha and S. Ulukus, "Optimization of cdma signature sequences in multipath channels,," in *IEEE VTS 53rd Vehicular Technology Conference*, vol. 3, 2001, pp. 1978 –1982.
- [13] L. Gao and T. Wong, "Sequence optimization in cdma point-to-point transmission with multipath," in *IEEE 56th Vehicular Technology Conference*, vol. 4, 2002, pp. 2303–2307.
- [14] M. Wrulich, C. Mehlfuhrer, and M. Rupp, "Managing the interference structure of mimo hsdpa: A multi-user interference aware mmse receiver with moderate complexity," *IEEE Transactions on Wireless Communications*, vol. 9, no. 4, pp. 1472 –1482, 2010.
- [15] A. Paulraj, R. Nabar, and D. Gore, *Introduction to Space-Time Wireless Communications*, 1st ed. Cambridge: Cambridge University Press, 2008.
- [16] H. A. G. M. K. Gurcan, I. Ma, "The interference-reduced energy loading for multi-code hsdpa systems," *EURASIP Journal on Wireless Communications and Networking*, 2012.

-
- [17] L. Maillaender, “Linear mimo equalization for cdma downlink signals with code reuse,” *IEEE Transactions on Wireless Communications*, vol. 4, no. 5, pp. 2423–2434, 2005.
- [18] R. Visoz, N. Gresset, and A. O. Berthe, “Advanced transceiver architectures for downlink mimo cdma evolution,” *IEEE Transactions on Wireless Communications*, vol. 6, no. 8, pp. 3016–3027, 2007.
- [19] K. Kiiskila, K. Hooli, J. Ylioinas, and M. Juntti, “Interference resistant receivers for wcdma mimo downlink,” in *IEEE 61st Vehicular Technology Conference*, vol. 2, VTC 2005 2005, 2005.
- [20] B. Kim, X. Zhang, and M. Flury, “Linear mmse space-time equalizer for mimo multicode cdma systems,” *IEEE Transactions on Communications*, vol. 54, no. 10, pp. 1710–1714, 2006.
- [21] S. Kim, S. Kim, C. Shin, J. Lee, and Y. Kim, “A new multicode interference cancellation method for hsdpa system,” *IEEE Pacific Rim Conference on Communications, Computers and Signal Processing*, pp. 487–490, 2009.
- [22] Z. He, M. Gurcan, and H. Ghani, “Time-efficient resource allocation algorithm over hsdpa in femtocell networks,” *2010 IEEE 21st International Symposium, Personal, Indoor and Mobile Radio Communications Workshops (PIMRC Workshops)*, pp. 197–202, 2010.
- [23] T. Bogale, L. Vandendorpe, and B. Chalise, “Robust transceiver optimization for downlink coordinated base station systems: distributed algorithm,” *IEEE Trans. Signal Process.*, vol. 60, no. 1, pp. 337–350, 2011.
- [24] M. Gurcan, “Presentation 4, mobile radio communications course,” Imperial College London, 2012.